Photoinduced Electron-Transfer Reactions with Quinolinic and Trimellitic Acid Imides: Experiments and Spin Density Calculations[1]

Axel G. Griesbeck,*[,†] Murthy S. Gudipati,*[,‡] Joachim Hirt,[†,§] Johann Lex,[†] Michael Oelgemöller,[†,||] Hans Schmickler,[†] and Frank Schouren[‡]

Institute of Organic Chemistry, University of Cologne, Greinstr. 4, Germany, and Institute of Physical Chemistry, University of Cologne, Luxemburgerstr. 116, D-50939 Köln, Germany

griesbeck@uni-koeln.de

Received July 17, 2000

The regioselectivity of photoinduced electron-transfer (PET) reactions of unsymmetrical phthalimides is controlled by the spin density distribution of the intermediate radical anions. ROHF ab initio calculations were found to be most suitable for atomic spin density analysis. *Intramolecular* PET reactions of quinolinic acid imides were studied with the potassium butyrate and hexanoate **1a**,**b** and a cysteine derivative **3**. The photocyclizations products **2a**,**b** and **4** were formed with moderate regioselectivities (68:32, 57:43, and 81:19) showing preferential ortho cyclization. The *intermolecular* reaction of potassium propionate and potassium isobutyrate with *N*-methylquinolinic acid imide (**5**) yielded as addition products the dihydropyrrolo[3,4-*b*]pyridines **6a**,**b** with slight ortho regioselectivity (55:45). In contrast to these low regioselectivities, the PET reaction of potassium propionate with the methyl ester of *N*-methyltrimellitic acid imide (**9**) yielded solely the para addition product **10**. Likewise, the *intramolecular* photoreaction of the cysteine derivative **7** gave a 75:25 (para/meta) mixture of regioisomeric cyclization products **8**. The regioselectivity originates from donor−acceptor interactions prior to electron transfer and differences in spin densities in the corresponding imide radical anions. The results of DFT and ab initio calculations for the radical anions of the quinolinic acid imide (**11**$^{\bullet-}$) and the methyl ester of trimellitic acid imide (**12**$^{\bullet-}$) were in agreement with the latter assumption: spin densities in **11**$^{\bullet-}$ were higher for the imido ortho carbon atoms (indicating preferential ortho coupling); for **12**$^{\bullet-}$ the spin densities were higher for the imido para carbon atoms (indicating preferential para coupling). These correlations became more significant when the additional spin densities at the carbonyl oxygen and the adjacent carbon atoms were taken into account. The cyclization selectivities for **2**, **4**, and **8** deviate from the intermolecular examples probably because of ground-state and solvent effects.

Introduction

We have intensively explored the photochemical[2] and photophysical properties[3] of phthalimides over the last years and developed a variety of synthetic applications for transformations of natural amino acids.[4] Especially promising were photoinduced electron-transfer (PET) cyclizations of acceptor−donor couples with the phthalimide chromophor serving as electron acceptor (E_{red} ca. −1.4 V vs SCE, excitation energies of 3.5 and 3 eV for the first excited singlet and triplet, respectively). As electron donors thioether[5] and carboxylate groups were investigated.[6] In the former cases, the electron donor becomes part of the newly formed ring system; in the latter case, decarboxylation and radical combination lead to the photoproduct. This method is widely applicable, and a multitude of medium and macrocyclic ring systems can be synthesized.[7] Additionally, an intermolecular modification of this reaction was developed[8] which allows the generation of carbon radicals in aqueous solution even under large-scale conditions using a 308 nm XeCl radiation reactor.[9]

Especially interesting substrates in this context are unsymmetrically substituted phthalimides that allow regioselectivity studies concerning inter- and intramolecular C−C coupling steps which may shed further light on the mechanism of the product-forming step and the spin density composition of intermediate radicals or radical ions. To the best of our knowledge, only a few examples for the photochemistry of unsymmetrically substituted phthalimide derivatives were reported in the

† Institute of Organic Chemistry.
‡ Institute of Physical Chemistry.
§ Present address: Novartis Pharma GmbH, Nürnberg, Germany.
|| Present address: Inoue Photochirogenesis Project, Toyonaka 560-0085, Japan.

(1) Parts of the doctoral thesis of J.H., University of Würzburg, 1995, and M.O., University of Cologne, 1999.
(2) Griesbeck, A. G. *Liebigs Ann. Chem.* **1996**, 1951−1958.
(3) Griesbeck, A. G.; Görner, H. *J. Photochem. Photobiol. A: Chem.* **1999**, *129*, 111−119.
(4) (a) Griesbeck, A. G. *Chimia* **1998**, *52*, 272−283. (b) Griesbeck, A. G. *EPA Newsletters* **1998**, 3−22.
(5) (a) Griesbeck, A. G.; Hirt, J.; Kramer, W.; Dallakian, P. *Tetrahedron* **1998**, *54*, 3169−3180. (b) Griesbeck, A. G.; Hirt, J.; Peters, K.; Peters, E.-M.; von Schnering, H. G. *Chem. Eur. J.* **1996**, *2*, 1388−1394.
(6) Griesbeck, A. G.; Kramer, W.; Oelgemöller, M. *Synlett* **1999**, 1169−1178.
(7) (a) Griesbeck, A. G.; Nerowski, F.; Lex, J. *J. Org. Chem.* **1999**, *64*, 5213−5217. (b) Griesbeck, A. G.; Henz, A.; Kramer, W.; Lex, J.; Nerowski, F.; Oelgemöller, M.; Peters, K.; Peters, E.-M. *Helv. Chim. Acta* **1997**, *80*, 912−933.
(8) (a) Griesbeck, A. G.; Oelgemöller, M. *Synlett* **1999**, 492−494. (b) Griesbeck, A. G.; M. Oelgemöller, M. *Synlett* **2000**, 71−72.
(9) Griesbeck, A. G.; Kramer, W.; Oelgemöller, M. *Green Chem.* **1999**, *1*, 205−207.

10.1021/jo001070r CCC: $19.00
Published on Web 09/22/2000

Scheme 1. Decarboxylative Photocyclization of 1a and 1b

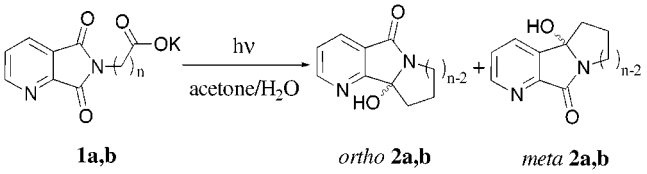

1a,b *ortho* **2a,b** *meta* **2a,b**

literature.[10] The results of these photochemical reactions can be compared with ground-state nucleophilic additions, e.g., the Grignard additions toward quinolinic acid imides.[11] The comparison of intramolecular reactions (either cyclization via thioether oxidation or photodecarboxylation) with intermolecular reactions (photodecarboxylative addition of carbon radicals to imides) should additionally disclose preorientation phenomena in the ground states.

Results and Discussion

The starting materials **1a**,**b** and the free imido-protected cysteine derivatives (precursors to **3** and **7**) were easily available in good yields from the corresponding amino acids according to a method described by Kidd and King.[12] The methyl esters **3**, **7**, and **9** were synthesized by standard procedures from the corresponding free acids.[5] *N*-Methylquinolinic acid imide **5** and *N*-methyltrimellitic acid imide (precursor to **9**) were synthesized according to Hemmerich[13] and Schindlbauer,[14] respectively.

Quinolinic Acid Imides. The potassium salts of the quinolinic acid imides **1a** and **1b** were irradiated at 300 nm in a 1:1 (vol. %) water/acetone mixture until complete conversion of the starting materials (Scheme 1). The photocyclization products **2a**,**b** were detected in the crude reaction mixture as sole products and could be isolated after recrystallization from acetone in 76% and 68% yield, respectively. The regioselectivity for both transformations was moderate favoring the ortho isomers (ortho and meta with respect to the pyridine nitrogen relative to the "reactive" carbonyl group) with regioselectivities of 68:32 and 57:43, respectively. The constitution of ortho and meta photocyclization products could not be determined unambiguously by NMR techniques. The definite proof was obtained from the X-ray structure analysis of the major regioisomer of **2a,** which is shown in Figure 1.[15]

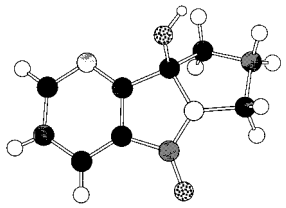

Figure 1. Crystal structure of *o*-**2a**.[15]

Scheme 2. Photocyclization of 3

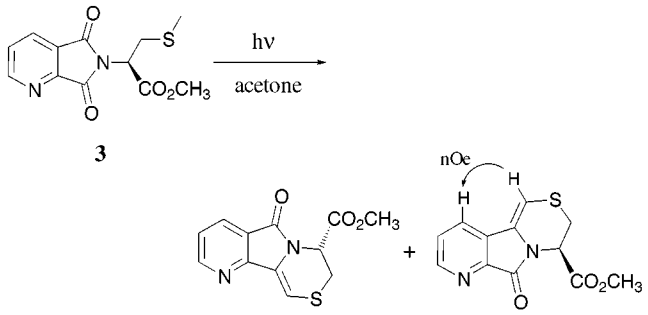

3 *ortho* **4** *meta* **4**

Table 1. Intra- versus Intermolecular Photoreactions in the Quinolinic Acid Series: Product Composition[a]

substrate	*n* or R	yield (%)	ortho (%)	meta (%)
1a	3	76 (**2a**)	68	32
1b	5	68 (**2b**)	57	43
3		67 (**4**)	81	19
5	Et	72 (**6a**)	55	45
5	^{i}Pr	78 (**6b**)	55	45

[a] Determined by ^{1}H NMR (±5%).

Next, the photocyclization of quinolinic acid imides was studied with the cysteine derivative **3** as a model substrate with an easily oxidizable thioether group. Irradiation ($\lambda = 300$ nm) in acetone resulted in a crude product mixture that could not be analyzed by NMR due to multiple overlapping signals. To reduce the spectral complexity, catalytic amounts of trifluoroacetic acid were added, and the resulting pyridinium salts were neutralized and isolated as the free bases **4**. These dehydration products can be clearly distinguished by the olefinic proton at 6.34 ppm (*meta*-**4**) and at 6.79 ppm (*ortho*-**4**). Complementary nuclear Overhauser enhancements (NOE) corroborated the spectral assignments for the two regioisomeric structures (Scheme 2). The regioisomers were formed in a 81:19 ratio with *ortho*-**4** as the major product analogous to the photodecarboxylation reaction of **1a**,**b** (Table 1).

To determine the regioselectivity of the radical combination step in the absence of possible ground-state interactions between the pyridine and the carboxylate group, we investigated the intermolecular photodecarboxylative addition of alkyl carboxylates with *N*-methylquinolinic acid imide (**5**). To check for steric effects, potassium propionate and isobutyrate were applied as radical precursors. Irradiation of **5** in a 4:1 acetone–water mixture in the presence of 5 equiv of the respective potassium carboxylate led to the addition products **6a** and **6b** in 72% and 78% yield (Scheme 3). There was only a slight preference for formation of the ortho isomer (55:45 regioisomeric ratio), and no steric effects were observed from the two radical precursors (Table 1). Thus,

(10) (a) Coyle, J. D., Bryant; L. R. B.; Cragg, J. E.; Challinger, J. F.; Haws, E. J. *J. Chem. Soc., Perkin Trans. 1* **1985**, 1177–1180. (b) Mazzocchi, P. H.; Khachik, F. *Tetrahedron Lett.* **1983**, *24*, 1879–1882. (c) Mazzocchi, P. H.; Khachik, F. *Tetrahedron Lett.* **1981**, *22*, 4189–4192.

(11) (a) Bahajaj, A. A.; Vernon, J. M. *J. Chem. Soc., Perkin Trans. 1* **1996**, 1041–1046. (b) Bahajaj, A. A.; Hitchings, G. J.; Moore, M. H.; Vernon, J. M. *J. Chem. Soc. Perkin Trans. 1* **1994**, 1211–1214. (c) Hitchings, G. J.; Vernon, J. M. *J. Chem. Soc., Perkin Trans. 1* **1990**, 1757–1763.

(12) Kidd, D. A. A.; King, F. E. *Nature* **1948**, *162*, 776.

(13) Hemmerich, P.; Fallab, S. *Helv. Chim. Acta* **1958**, *41*, 498–513.

(14) Schindlbauer, H. *Monatsh. Chem.* **1973**, *104*, 848–853.

(15) The crystals of *ortho*-**2a** ($C_{10}H_{10}N_2O_2$, $M = 190.20$, from acetone/*n*-hexane) are monoclinic, space group $P2_1$, $a = 768.9(1)$ pm, $b = 652.4(1)$ pm, $c = 908.7(1)$ pm; $\beta = 101.48(1)°$; $V = 446.7(1) \times 10^6$ pm^3; $Z = 2$; $d_{calc} = 1.414$ g/cm^3. Data collection: Enraf-Nonius CAD4-diffractometer, Mo Kα, graphite monochromator, Wyckoff-scan, theta range (deg): 2.29–26.30, crystal dimensions: 0.25 × 0.2 × 0.2 mm; no. reflns measd: 1810, no. unique refl.: 1775, no. refl. $F > 2\sigma(F)$: 622; R, R_w: 0.037, 0.084.

Scheme 3. Decarboxylative Photoaddition of Alkylcarboxylates to 5

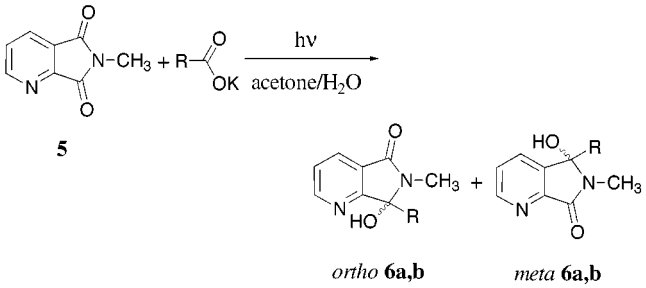

Table 2. Intra- versus Intermolecular Photoreactions in the Trimellitic Acid Series: Product Composition[a]

substrate	R	yield (%)	para (%)	meta (%)
7		66 (**8**)	75	25
9	Et	84 (**10**)	>95	<5

[a] Determined by ^{1}H NMR (±5%).

Scheme 4. Photocyclization of 7

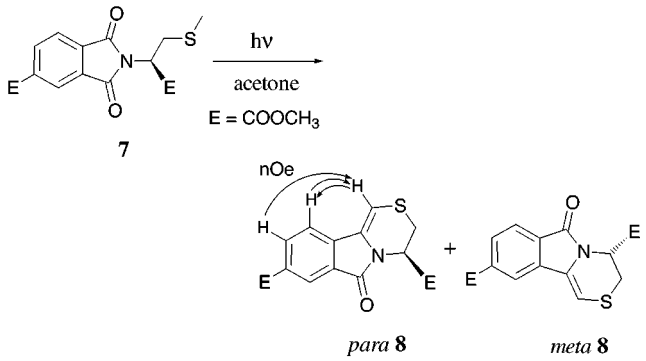

ground-state interactions in the photodecarboxylation reaction of **1a**,**b** are unlikely.

Trimellitic Acid Imides. The second group with unsymmetrical chromophors were the trimellitic acid imide derivatives **7** and **9**. The redox potentials measured for the cysteine derivative **7** were −1.20 V (reversible) and +1.6 V (irreversible, anodic onset). The corresponding phthalimide showed an identical oxidation potential and a slightly shifted reduction potential of −1.43 V (reversible, all values vs Ag/AgCl). After irradiation of **7** in acetone and treatment with catalytic amounts of trifluoroacetic acid (vide supra), a 75:25 mixture of regioisomeric cyclization products **8** was isolated in 67% yield (Table 2, Scheme 4). Strong NOE enhancements measured for the major component established its para constitution.

To determine the regioselectivity of the radical combination step in the absence of ground-state interactions also for the trimellitic acid case, we investigated the intermolecular photodecarboxylative addition of potassium propionate with *N*-methyltrimellitic acid imide (**9**). Irradiation of **9** in a 4:1 acetone−water mixture in the presence of 5 equiv of the potassium salt of propionic acid led to the addition product **10** in 84% yield (Table 2, Scheme 5). In the crude product mixture only one set of signals was detected in proton and carbon NMR. The para constitution of adduct **10** was unambiguously determined by ROESY[16] spectroscopy (Figure 2). Thus,

(16) Rotating frame Overhauser Effect Spectroscopy (ROESY): Bax, A.; Davis, D. G. *J. Magn. Reson.* **1985**, *63*, 207−213.

Scheme 5. Decarboxylative Addition of Propionate to 9

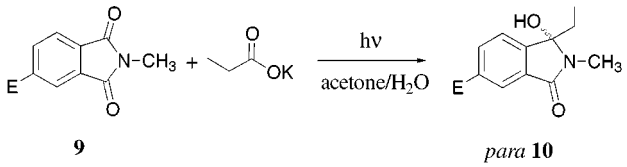

Scheme 6. Proposed Reaction Mechanism

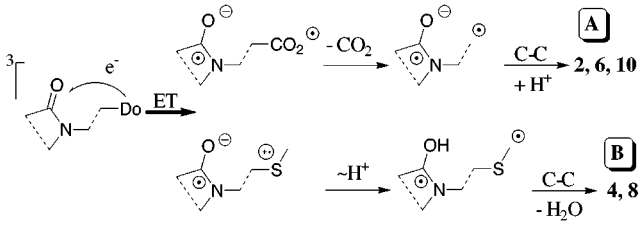

the intermolecular reaction is highly regioselective in contrast to the intramolecular cyclization of the cysteine substrate **7**.

Proposed Reaction Mechanism: Computations. The key step in the intra- and intermolecular reactions of the substrates reported herein is the photoinduced electron transfer from the donor group to the triplet excited imide.[5,6] Electron-transfer route **A** generates a carboxyl radical that subsequently undergoes CO_2 extrusion and C−C coupling (after intersystem crossing of the triplet biradical or triplet radical cage pair, respectively) to give products **2**, **6**, and **10** as the respective potassium alkoxides (Scheme 6). In route **B**, a triplet radical ion pair is formed with a sulfur-centered radical cation which subsequently undergoes proton transfer from the terminal α-position with respect to the sulfur atom, intersystem crossing, and C−C coupling to give the products **4** and **8**.

When applying these mechanistic pictures, the relative atomic spin densities of the reactive carbonyl carbons of the intermediate radical anions are expected to be an useful index for the regioselectivity of the radical coupling steps.[17] We have thus performed a series of calculations on the radical anions of quinolinic acid imide **11**$^{\bullet-}$ and the methyl ester of trimellitic acid imide **12**$^{\bullet-}$ (Figure 3).

Several recent publications dealing with experimental and theoretical investigations on radical ions unanimously conclude that the DFT method (B3LYP functional) predicts the hyperfine coupling constants as well as the atomic spin densities satisfactorily.[18−20] In one paper where different computational methods have been compared among each other and with experimental data, it was noted that the spin densities computed using the ROHF method reproduces the experimental spin densities of the radical anion of para-benzoquinone extremely well.[19] At the same time, it was noted that due to the fact that the ROHF method includes neither spin polar-

(17) (a) Freccera, M.; Fasani, E.; Albini, A. *J. Org. Chem.* **1993**, *58*, 1740−1745; (b) Kubo, Y.; Nanba, M.; Hayashi, E.; Araki, T. *Bull. Chem. Soc. Jpn.* **1989**, *62*, 3972−3977.

(18) (a) Niemz, A.; Rotello, V. M. *J. Am. Chem. Soc.* **1997**, *119*, 6833−6836. (b) Mariam, Y. H.; Chantranupong, L. *J. Comput.-Aided Mol. Design* **1997**, *11*, 345−356. (c) Wheeler, D. A.; Rodriguez, J. H.; McCusker, J. K. *J. Phys. Chem. A* **1999**, *103*, 4101−4112. (d) O'Malley, P. J. *J. Phys. Chem. A* **1997**, *101*, 9813−9817.

(19) Boesch, S. E.; Wheeler, R. A. *J. Phys. Chem. A* **1997**, *101*, 8351−8359.

(20) Yamauchi, J.; Fujita, H. *Bull. Chem. Soc. Jpn.* **1993**, *66*, 2505−2509.

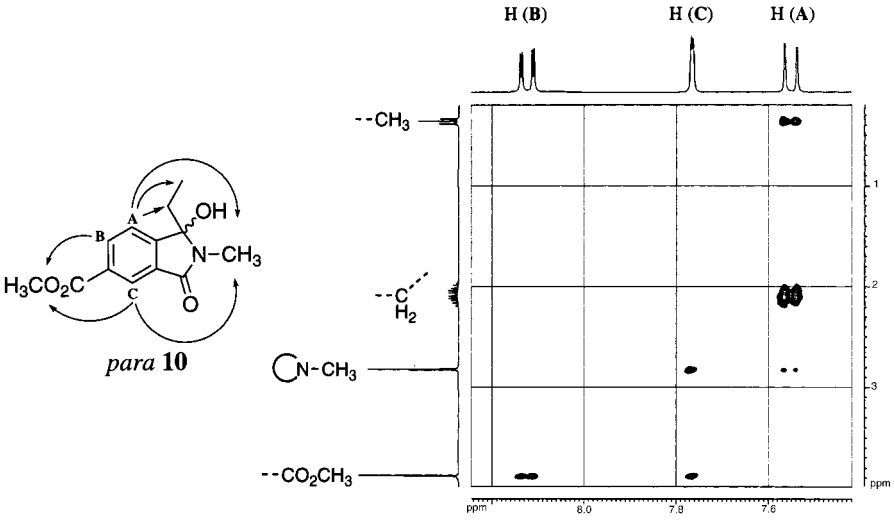

Figure 2. ROESY spectrum and NOE enhancements for *p*-**10**.

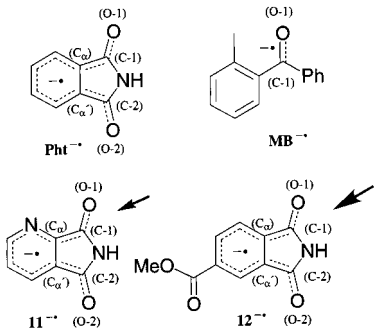

Figure 3. Relevant atomic positions in **Pht**$^{\bullet-}$, **MB**$^{\bullet-}$, **11**$^{\bullet-}$, and **12**$^{\bullet-}$ (arrows indicate preferred site of radical addition).

izations nor correlation effects, the observed agreement should almost be fortuitous. On the other hand, the QCISD (configuration interaction using single, double, and quadruple excitations) ab initio method as well as B3LYP functional in the DFT method have been suggested in the GAUSSIAN98 handbook to predict spin densities of radical anions satisfactorily.

With this background in mind, we have decided to carry out computations of the atomic spin densities using DFT, ROHF, and QCISD methods. Spin densities have additionally been calculated for the 2-methylbenzophenone radical anion (**MB**$^{\bullet-}$) for which experimental values have been published.[20] The results of these calculations are summarized in Table 3. Geometries of the radical anions were optimized using the same method, basis set, and functional before computing spin densities.

All three types of computations, namely DFT (BLYP, B3LYP), ROHF, and QCISD, are in agreement among each other with the qualitative trend of relative localization of the atomic spin densities and consequently the regioselectivities observed for the C−C radical coupling reactions of quinolinic and trimellitic acid imides. This observation is, however, only valid for the triads of reactive carbon atoms C-1, C-2 plus the adjacent oxygen atoms O-1, O-2 and the α-carbon positions C_α and C_α'. A more detailed analysis of (i) the internal relative atomic spin distribution and (ii) the comparative spin densities between the reactive carbonyl groups revealed, that the QCISD method for **11**$^{\bullet-}$ strongly overestimates the spin density at oxygen and predicts anomalous small spin densities at the carbonyl carbon atoms. Consequently, no further calculations were performed with this expensive method. The DFT calculation which has been described as a reliable method for spin density calculations also yields higher spin densities for oxygen. These observations are in agreement with the results for other radical anions using DFT methods. An increase in basis set size even amplifies this trend. On the other hand, the ROHF calculations reproduce the closest the experimental values for **MB**$^{\bullet-}$ concerning total spin density and spin density distribution and gave realistic values also in comparison with the experimental values for the symmetric **Pht**$^{\bullet-}$.[23]

From these calculations and the comparison with the literature values for **MB**$^{\bullet-}$ we conclude that the results of the ROHF calculations are best suitable for mechanistic interpretations (entries 6, 7 and 13, 14, respectively). Thus, the reactivity differences between the two imido carbonyl groups in **11**$^{\bullet-}$ and **12**$^{\bullet-}$ are expected to

Table 3. Atomic Spin Densities in 11$^{\bullet-}$, 12$^{\bullet-}$, and MB$^{\bullet-}$

	(C-1)	(O-1)	(C_α)	(C-2)	(O-2)	(C_α')
Pht$^{\bullet-}$expt[23]	0.174	0.054	0.187	0.174	0.054	0.187
11$^{\bullet-}$DFT[a]	0.105	0.188	0.221	0.099	0.159	0.159
11$^{\bullet-}$DFT[b]	0.111	0.175	0.200	0.106	0.152	0.147
11$^{\bullet-}$DFT[c]	0.121	0.182	0.168	0.100	0.155	0.164
11$^{\bullet-}$DFT[d]	0.126	0.169	0.151	0.109	0.149	0.153
11$^{\bullet-}$HF[e]	0.158	0.107	0.293	0.081	0.053	0.134
11$^{\bullet-}$HF[f]	0.175	0.099	0.309	0.077	0.046	0.120
11$^{\bullet-}$QCISD	−0.021	0.324	0.364	0.064	0.237	0.189
12$^{\bullet-}$DFT[a]	0.080	0.163	0.250	0.051	0.096	0.084
12$^{\bullet-}$DFT[b]	0.089	0.149	0.222	0.059	0.090	0.067
12$^{\bullet-}$DFT[c]	0.075	0.159	0.204	0.080	0.095	0.073
12$^{\bullet-}$DFT[d]	0.087	0.146	0.185	0.085	0.089	0.057
12$^{\bullet-}$HF[e]	0.123	0.086	0.309	0.042	0.033	0.098
12$^{\bullet-}$HF[f]	0.134	0.078	0.303	0.040	0.030	0.107
MB$^{\bullet-}$DFT[a]	0.217	0.280				
MB$^{\bullet-}$DFT[b]	0.198	0.255				
MB$^{\bullet-}$DFT[c]	0.082	0.259				
MB$^{\bullet-}$DFT[d]	0.073	0.235				
MB$^{\bullet-}$HF[e]	0.346	0.248				
MB$^{\bullet-}$HF[f]	0.325	0.188				
MB$^{\bullet-}$exp.[20]	0.458	0.113				

[a] B3LYP, G-31G(d). [b] BLYP, G-31G(d). [c] B3LYP, G-311G++(d,p). [d] BLYP, G-311G++(d,p). [e] ROHF, G-31G(d). [f] ROHF, G-311G++(d,p).

(21) Yoon, U. C.; Oh, S. W.; Lee, S. M.; Cho, S. J.; Gamlin, J.; Mariano, P. S. *J. Org. Chem.* **1999**, *64*, 4411−4418.

be significant with preferential formation of ortho (from **11**$^{\bullet-}$) and para (from **12**$^{\bullet-}$) adducts, respectively. This is in accord with the results of the intramolecular PET reactions of the cysteine derivatives **3** and **7**. The photocyclization reactions proceeded similarly with regioselectivities of 81:19 and 75:25, respectively. Albeit not directly comparable with gas-phase conditions, photolysis in acetone can be assumed to proceed without significant interactions with the solvent. In contrast to route **B** (Scheme 6), the intra- and intermolecular photodecarboxylation reactions (route **A**) are inefficient in the absence of water.[7b] Thus, additional interactions with the solvent have to be taken into account which were not considered in the present calculations. Solvent effects in photoinduced electron transfer processes of phthalimides have also been described recently by Mariano and coworkers.[21] In the case of the quinolinic acid imides the regioselectivity is strongly reduced in aqueous solvents in intra- as well as intermolecular PET reactions whereas the regioselectivity of the alkylation reaction of the trimellitic acid imide **9** increases in comparison with the photocyclization of **3**. These effects can be interpreted as originating from hydrogen bonding interactions of the solvent molecules with the pyridine nitrogen of the quinolinic acid substrates (moderating spin density distribution) and the ester group of the trimellitic acid substrates (enhancing differences in spin density distribution), respectively.

Conclusions

The regioselectivity of PET reactions of unsymmetrical phthalimides is controlled by the spin density distribution of the intermediate radical anions. ROHF ab initio calculations are most suitable for predicting realistic atomic spin densities.

Experimental Section

The starting materials were synthesized from the amino acids and quinolinic acid or trimellitic acid anhydride according to Kidd.[12] The methyl esters were synthesized from the free acids using HCl gas saturated methanol as described by us earlier.[4] *N*-Methylquinolinic acid was obtained according to Hemmerich[15] and *N*-methyltrimellitic acid imide according to Schindlbauer.[16]

Computation of the atom spin densities of the radical anions of the quinolinic acid imide **11**$^{\bullet-}$, the methyl ester of trimellitic acid imide **12**$^{\bullet-}$, as well as 2-methylbenzophenone (**MB**$^{\bullet-}$) was performed using the quantum chemistry program Gaussian 98[22] on an SGI origin with 32 processors (R 12000) and 16 GB main memory. Computations were carried out with restricted open-shell HF (ROHF) as well as DFT methods (functionals: BLYP and B3LYP) using two split valence basis sets of different size, 6-31G(d) and G-311G++(d,p), in order to examine the effect of diffuse and additional polarization functions on the calculated properties. QCISD calculations were carried out only on **11**$^{\bullet-}$ with a smaller basis set (6-31G) without polarization or diffuse functions. The number of basis functions (bf) as well as the number of primitive Gaussians (pg) for each radical anion and basis set are given in Table 4.

Table 4. Number of Basis Functions (bf) and Primitive Gaussians (pg) for the Radical Anions and Basis Sets Used in Spin Density Calculations

	6-31G		6-31G(d)		6-311G++(d,p)	
radical anion	bf	pg	bf	pg	bf	pg
11$^{\bullet-}$	107	258	173	324	270	432
12$^{\bullet-}$			239	448	379	603
MB$^{\bullet-}$			249	468	414	648

The photochemical reactions were performed in Pyrex vessels (100−250 mL) using a RPR-208 Rayonet photochemical reactor equipped with 3000 Å lamps (λ = 300 nm ± 10 nm; approximately 800 W) at 15 °C under a nitrogen atmosphere. Acetone used for photoreactions was puriss. p.a. (Fluka). Analyses of the crude product mixtures were performed using ^{1}H and ^{13}C NMR spectroscopy. Analyses of the purified photoproducts were performed using ^{1}H and ^{13}C NMR, IR, and UV spectroscopy and mp and combustion analyses. CV: EG&G PAR 273 potentiostat, values in acetonitrile, TBAHFP as electrolyte.

Standard Procedure for the Synthesis of the *N*-Quinolinic Acid Imides and *N*-Trimellitic Acid Imides. Equimolar amounts of the amino acid and quinolinic acid anhydride or trimellitic acid anhydride, respectively, were heated in an open flask to 150 °C for about 45 min. After complete evaporation of the H_2O and cooling to ca. 50 °C, the mixture was poured into water. Filtration and recrystallization from acetone gave the desired products.

4-(5,7-Dioxo-5,7-dihydropyrrolo[3,4-*b*]pyridin-6-yl)butyric Acid (1a). From γ-amino butyric acid and quinolinic acid anhydride: beige solid (51%); mp 191−192 °C; ^{1}H NMR (300 MHz, $CDCl_3$/DMSO-d_6 (ca.10%)) δ 1.95 (tt, J = 6.9, 7.5 Hz, 2H), 2.28 (t, J = 7.5 Hz, 2H), 3.75 (t, J = 6.9 Hz, 2H), 7.55 (dd, J = 5.0, 7.7 Hz, 1H), 8.09 (dd, J = 7.7, 1.6 Hz, 1H), 8.88 (dd, J = 5.0, 1.6 Hz, 1H); ^{13}C NMR (75.5 MHz, $CDCl_3$/DMSO-d_6 (ca.10%)) δ 23.7 (t), 31.2 (t), 37.4 (t), 127.1 (s), 127.2 (d), 131.0 (d), 155.0 (d, s), 166.1 (2s), 174.4 (s). Anal. Calcd for $C_{11}H_{10}N_2O_4$: C, 56.41; H, 4.30; N, 11.96. Found: C, 56.48; H, 4.17; N, 12.12.

4-(5,7-Dioxo-5,7-dihydropyrrolo[3,4-*b*]pyridin-6-yl)hexanoic Acid (1b). From 6-aminohexanoic acid and quinolinic acid anhydride: beige solid (39%); mp 131−132 °C; ^{1}H NMR (300 MHz, $CDCl_3$/DMSO-d_6 (ca.10%)) δ 1.20 (m, 2H), 1.46 (m, 4H), 2.05 (t, J = 7.2 Hz, 2H), 3.52 (t, J = 7.2 Hz, 2H), 7.44 (dd, J = 5.0, 7.6 Hz, 1H), 7.96 (dd, J = 7.6, 1.5 Hz, 1H), 8.74 (dd, J = 5.0, 1.5 Hz, 1H); ^{13}C NMR (75.5 MHz, $CDCl_3$/DMSO-d_6 (ca.10%)) δ 23.9 (t), 25.8 (t), 27.7 (t), 33.4 (t), 37.5 (t), 126.8 (s), 127.0 (d), 130.7 (d), 154.6 (d,s), 165.6 (s), 165.9 (s), 175.0 (s). Anal. Calcd for $C_{13}H_{14}N_2O_4$: C, 59.54; H, 5.38; N, 10.68. Found: C, 59.32; H, 5.20; N, 10.91.

Standard Procedure for the Synthesis of the Methyl Esters. A stream of gaseous HCl was bubbled through a suspension of the N-protected *S*-methylcysteine in methanol for 2 min. After being cooled to 0 °C, the solution was again saturated with gaseous HCl for 2 min and stirred overnight at rt. The excess methanol was then removed by distillation under reduced pressure, and the oily residues were dried in vacuo. The products were obtained after column chromatography or recrystallization.

2-(5,7-Dioxo-5,7-dihydropyrrolo[3,4-*b*]pyridin-6-yl)-3-methylsulfanylpropionic Acid Methyl Ester (3). From cysteine in 32% yield: colorless liquid; ^{1}H NMR (300 MHz, $CDCl_3$) δ 2.05 (s, 3H), 3.32 (ddd, J = 6.0, 10.3, 14.5 Hz, 2H), 3.72 (s, 3H), 5.05 (dd, J = 6.0, 10.3 Hz, 1H), 7.62 (dd, J = 5.0, 7.7 Hz, 1H), 8.16 (dd, J = 1.5, 7.7 Hz), 8.96 (dd, J = 1.5, 5.0 Hz, 1H); ^{13}C NMR (75.5 MHz, $CDCl_3$): δ = 15.0 (q), 32.9 (t), 50.7 (q), 53.0 (d), 127.5 (d), 131.5 (d), 136.0 (s), 149.1 (s), 155.5 (d), 165.2 (s), 165.3 (s), 168.2 (s). Anal. Calcd for $C_{12}H_{12}N_2$-

(22) Frisch, M. J.; Trucks, G. W.; Schlegel, H. B.; Scuseria, G. E.; Robb, M. A.; Cheeseman, J. R.; Zakrzewski, V. G.; Montgomery, J. A. Jr.; Stratmann, R. E.; Burant, J. C.; Dapprich, S.; Millam, J. M.; Daniels, A. D.; Kudin, K. N.; Strain, M. C.; Farkas, O.; Tomasi, J.; Barone, V.; Cossi, M.; Cammi, R.; Mennucci, B.; Pomelli, C.; Adamo, C.; Clifford, S.; Ochterski, J.; Petersson, G. A.; Ayala, P. Y.; Cui, Q.; Morokuma, K.; Malick, D. K.; Rabuck, A. D.; Raghavachari, K.; Foresman, J. B.; Cioslowski, J.; Ortiz, J. V.; Baboul, A. G.; Stefanov, B. B.; Liu, G.; Liashenko, A.; Piskorz, P.; Komaromi, I.; Gomperts, R.; Martin, R. L.; Fox, D. J.; Keith, T.; Al-Laham, M. A.; Peng, C. Y.; Nanayakkara, A.; Challacombe, M.; Gill, P. M. W.; Johnson, B.; Chen, W.; Wong, M. W.; Andres, J. L.; Gonzalez, C.; Head-Gordon, M.; Replogle, E. S.; Pople, J. A. Gaussian 98, Revision A.7; Gaussian Inc., Pittsburgh, PA, ***1998***.

(23) Sioda, R. E.; Koski, W. S. *J. Am. Chem. Soc.* **1967**, *89*, 475.

SO_4: C, 51.42; H, 4.32; N, 9.99; S, 11.49. Found: C, 51.23; H, 4.02; N, 10.26; S, 10.97.

2-Methyl-1,3-dioxo-2,3-dihydro-1*H*-isoindole-5-carboxylic Acid Methyl Ester (7). From cysteine in 23% yield: colorless liquid; UV (CH_3CN) λ_{max} (ϵ) = 299.0 nm (2482) 255.0 (45055); ^{1}H NMR (300 MHz, $CDCl_3$) δ 2.11 (s, 3H), 3.36 (dd, J = 9.8, 10.6 Hz, 2H), 3.78 (s, 3H), 4.00 (s, 3H), 5.05 (dd, J = 6.4, 9.8 Hz, 1H), 7.97 (dd, J = 0.7, 7.8 Hz, 1H), 8.45 (dd, J = 1.4, 7.8 Hz, 1H), 8.52 (dd, J = 0.7, 1.3 Hz, 1H); ^{13}C NMR (75.5 MHz, $CDCl_3$) δ 14.9 (q), 32.8 (t), 50.5 (d), 52.7 (q), 52.8 (q), 123.5 (d), 124.5 (d), 131.7 (s), 134.8 (s), 135.4 (d), 135.6 (s), 164.8 (s), 166.2 (s), 166.3 (s), 168.3 (s). Anal. Calcd for $C_{15}H_{15}NSO_6$: C, 53.41; H, 4.48; N, 4.15; S, 9.50. Found: C, 53.27; H, 4.72; N, 4.34; S, 9.33.

Standard Irradiation Procedures. Procedure A. An equimolar mixture of K_2CO_3 (1 mmol) and the substrate (2 mmol) in water (10 mL) and acetone (10 mL) was heated smoothly until the CO_2 extrusion had stopped. Additional water (50 mL) and acetone (130 mL) were added. A homogeneous solution resulted that was irradiated for 12−24 h while purging with a slow stream of nitrogen. The residual solution was extracted with CH_2Cl_2 (3 × 100 mL), washed with 5% $NaHCO_3$ and brine, dried ($MgSO_4$), and evaporated to dryness. The products were obtained after recrystallization from acetone.

2a. This compound was detected in the proton NMR spectrum as a mixture of the regioisomers *ortho*/*meta*-**2a**: colorless crystals (76%); mp 163−165 °C. 3a-Hydroxy-1,2,3,-3a-tetrahydro-4,8a-diazacyclopenta[*a*]inden-8-one (*ortho*-**2a**): ^{1}H NMR (300 MHz, $CDCl_3$): δ = 1.58 (ddd, J = 12.3, 8.8, 12.3 Hz, 1H), 2.22−2.42 (br m, 2H), 2.65 (m, 1H), 3.45 (ddd, J = 11.9, 9.4, 2.9 Hz, 1H), 3.64 (ddd, J = 11.9, 11.2, 8.4 Hz, 1H), 5.22 (br s, 1H), 7.33 (dd, J = 7.5, 5.1 Hz, 1H), 7.90 (dd, J = 7.5, 1.1 Hz, 1H), 8.54 (dd, J = 5.1, 1.1 Hz, 1H); ^{13}C NMR (75.5 MHz, $CDCl_3$): δ = 27.3 (t), 34.0 (t), 41.7 (t), 96.0 (s), 124.5 (d), 132.4 (d), 141.8 (s), 152.5 (d), 165.5 (s), 167.5 (s).

3a-Hydroxy-1,2,3,3a-tetrahydro-7,8a-diazacyclopenta[*a*]inden-8-one (*meta*-**2a**): ^{1}H NMR (300 MHz, $CDCl_3$) δ 1.48 (ddd, J = 11.9, 11.9, 8.8 Hz, 1H), 2.22−2.42 (br m, 2H), 2.68 (m, 1H), 3.41 (m, 1H), 3.64 (m, 1H), 4.84 (br s, 1H), 7.33 (m, 1H), 7.90 (m, 1H), 8.52 (m, 1H); ^{13}C NMR (75.5 MHz, $CDCl_3$) δ 27.3 (t), 34.7 (t), 41.5 (t), 94.1 (s), 125.9 (d), 126.1 (d), 131.0 (s), 149.8 (s), 151.5 (d), 167.6 (s). Anal. Calcd for $C_{10}H_{10}N_2O_2$ (diastereoisomeric mixture): C, 63.15; H, 5.30; N, 14.73. Found: C, 63.33; H, 4.97; N, 15.04.

2b. This compound was detected in the proton NMR spectrum as a mixture of the regioisomers *ortho*/*meta*-**2b**: beige solid (68%); mp 147−153 °C. 4b-Hydroxy-4b,5,6,7,8,9-hexahydro-4,9a-diazabenzo[*a*]azulen-10-one (*ortho*-**2b**): ^{1}H NMR (300 MHz, $CDCl_3$) δ 0.59 (dd, J = 24.2, 12.1 Hz, 1H), 1.10−1.41 (br m, 2H), 1.49−1.68 (br m, 3H), 2.03 (dd, J = 14.7, 11.2 Hz, 1H), 2.65 (dd, J = 14.7, 7.9 Hz, 1H), 3.10 (m, 1H), 3.67 (m, 1H), 5.51 (br s, 1H), 7.23 (dd, J = 7.7, 4.8 Hz, 1H), 7.73 (d, J = 7.7 Hz, 1H), 8.51 (d, J = 4.8 Hz, 1H); ^{13}C NMR (75.5 MHz, $CDCl_3$) δ 22.2 (t), 26.9 (t), 29.6 (t), 36.9 (t), 38.9 (t), 89.1 (s), 123.9 (d), 131.0 (d), 142.1 (s), 152.4 (d), 165.5 (s), 165.8 (s).

4b-Hydroxy-4b,5,6,7,8,9-hexahydro-1,9a-diazabenzo[*a*]azulen-10-one (*meta*-**2b**): ^{1}H NMR (300 MHz, $CDCl_3$) δ 0.59 (dd, J = 24.2, 12.1 Hz, 1H), 1.10−1.41 (br m, 2H), 1.49−1.68 (br m, 3H), 2.03 (dd, J = 14.7, 11.2 Hz, 1H), 2.40 (dd, J = 14.9, 8.1 Hz, 1H), 3.10 (m, 1H), 3.67 (m, 1H), 5.51 (br s, 1H), 7.29 (dd, J = 7.7, 5.0 Hz, 1H), 7.80 (d, J = 7.7 Hz, 1H), 8.39 (d, J = 5.0 Hz, 1H); ^{13}C NMR (75.5 MHz, $CDCl_3$) δ 22.0 (t), 26.8 (t), 29.4 (t), 38.2 (t), 38.8 (t), 90.8 (s), 125.0 (d), 130.3 (d), 149.5 (s), 150.9 (d), 165.2 (s), 165.8 (s). Anal. Calcd for $C_{12}H_{14}N_2O_2$ (diastereoisomeric mixture) C, 66.04; H, 6.47; N, 12.84. Found: C, 66.32; H, 6.61; N, 13.11.

Procedure B. The *N*-methylimide (2 mmol) was dissolved in 240 mL of acetone. A solution of the potassium carboxylate (10 mmol) in 60 mL of water was added and the mixture was irradiated for 12−24 h while purging with a slow stream of N_2. The solution was extracted with CH_2Cl_2 (3 × 100 mL), washed with 5% $NaHCO_3$ and brine, dried over $MgSO_4$, and evaporated to dryness. The products were obtained after drying in vacuo.

6a. This compound was detected in the proton NMR spectrum as a mixture of the regioisomers *ortho*/*meta*-**6a**: orange oil (72%). 7-Ethyl-7-hydroxy-6-methyl-6,7-dihydropyrrolo[3,4-*b*]pyridine-5-one (*ortho*-**6a**): ^{1}H NMR (300 MHz, $CDCl_3$) δ 0.43 (t, J = 7.4 Hz, 3H), 2.08 (qd, J = 14.3, 7.4 Hz, 1H), 2.39 (qd, J = 14.3, 7.4 Hz, 1H), 2.96 (s, 3H), 7.34 (dd, J = 4.9, 7.7 Hz, 1H), 7.93 (dd, J = 7.7, 1.4 Hz, 1H), 8.65 (dd, J = 4.9, 1.4 Hz, 1H); ^{13}C NMR (75.5 MHz, $CDCl_3$) δ 7.8 (q), 23.5 (q), 27.7 (t), 91.2 (s), 124.5 (d), 125.9 (s), 131.5 (d), 152.7 (d), 165.2 (s), 165.6 (s).

5-Ethyl-5-hydroxy-6-methyl-5,6-dihydropyrrolo[3,4-*b*]pyridine-7-one (*meta*-**6a**): ^{1}H NMR (300 MHz, $CDCl_3$) δ 0.47 (t, J = 7.5 Hz, 3H), 2.08 (m, 1H), 2.15 (m, 1H), 2.89 (s, 3H), 7.36 (dd, J = 5.1, 7.8 Hz, 1H), 7.85 (dd, J = 7.8, 1.3 Hz, 1H), 8.54 (dd, J = 5.1, 1.3 Hz, 1H); ^{13}C NMR (75.5 MHz, $CDCl_3$) δ 7.8 (q), 23.5 (q), 28.3 (t), 89.8 (s), 126.1 (d), 130.5 (d), 140.8 (s), 150.2 (s), 151.6 (d), 165.5 (s). Anal. Calcd for $C_{10}H_{12}N_2O_2$ (diastereoisomeric mixture): C, 62.49; H, 6.29; N, 14.57. Found: C, 62.41; H, 6.14; N, 14.74.

6b. This compound was detected in the proton NMR spectrum as a mixture of the regioisomers *ortho*/*meta*-**6b**: orange oil (78%). 7-Hydroxy-7-isopropyl-6-methyl-6,7-dihydropyrrolo[3,4-*b*]pyridine-5-one (*ortho*-**6b**): ^{1}H NMR (300 MHz, $CDCl_3$) δ 0.58 (d, J = 6.8 Hz, 3H), 1.24 (d, J = 6.8 Hz, 3H), 2.48 (sep., J = 6.8 Hz, 1H), 2.97 (s, 3H), 3.97 (br s, 1H), 7.29 (dd, J = 5.1, 7.6 Hz, 1H), 7.90 (dd, J = 7.6, 1.4 Hz, 1H), 8.58 (dd, J = 5.1, 1.4 Hz, 1H); ^{13}C NMR (75.5 MHz, $CDCl_3$) δ 16.4 (q), 16.7 (q), 23.8 (q), 33.6 (d), 92.1 (s), 124.2 (d), 126.0 (s), 131.1 (d), 151.9 (d), 164.7 (s), 165.4 (s).

5-Hydroxy-5-isopropyl-6-methyl-5,6-dihydropyrrolo[3,4-*b*]-pyridine-7-one (meta-**6b**): ^{1}H NMR (300 MHz, $CDCl_3$) δ 0.38 (d, J = 7.0 Hz, 3H), 1.14 (d, J = 7.0 Hz, 3H), 2.38 (sep., J = 7.0 Hz, 1H), 2.77 (s, 3H), 5.23 (br s, 1H), 7.22 (dd, J = 5.1, 7.7 Hz, 1H), 7.84 (dd, J = 7.7, 0.7 Hz, 1H), 8.38 (dd, J = 5.1, 0.7 Hz, 1H); ^{13}C NMR (75.5 MHz, $CDCl_3$) δ 16.2 (q), 17.2 (q), 23.5 (q), 33.4 (d), 91.3 (s), 125.2 (d), 131.6 (d), 139.6 (s), 150.1 (s), 150.9 (d), 165.0 (s). Anal. Calcd for $C_{11}H_{14}N_2O_2$ (diastereoisomeric mixture): C, 64.06; H, 6.84; N, 13.58. Found: C, 64.22; H, 7.01; N, 13.53.

3-Ethyl-3-hydroxy-2-methyl-2,3-dihydro-1*H*-isoindol-5-carbonic Acid Methyl Ester (*para*-10). This compound was detected as the sole product in the ^{1}H NMR spectrum of the crude reaction mixture: colorless liquid (84%); ^{1}H NMR (300 MHz, acetone-d_6) δ 0.39 (t, J = 7.4 Hz, 3H), 2.01 (qd, J = 14.3, 7.4 Hz, 1H), 2.14 (qd, J = 14.3, 7.4 Hz, 1H), 2.86 (s, 3H), 3.87 (s, 3H), 5.49 (s, 1H), 7.69 (d, J = 7.9 Hz, 1H), 8.04 (d, J = 0.9 Hz, 1H), 8.17 (dd, J = 7.9, 1.5 Hz, 1H); ^{13}C NMR (75.5 MHz, acetone-d_6) δ 7.9 (q), 23.2 (q), 29.1 (t), 52.6 (q), 91.5 (s), 123.1 (d), 123.9 (d), 132.0 (s), 133.2 (s), 133.7 (d), 152.1 (s), 166.1 (s), 166.3 (s). Anal. Calcd for $C_{13}H_{15}NO_4$: C, 62.64; H, 6.07; N, 5.62. Found: C, 62.43; H, 6.42; N, 5.53.

Procedure C. A solution of the substrate **3**, **7** (2 mmol) in acetone (200 mL) was irradiated for 12−24 h in a Pyrex vessel while being purged with a constant stream of dry nitrogen. After evaporation of ca. 80% of the solvent, catalytic amounts of trifluoroacetic acid were added. After the mixture was stirred for 1 h at rt, aqueous sodium bicarbonate solution was added and the product extracted with methylene chloride and purified by column chromatography.

Regioisomers **4**: 67% yield, colorless oil. 9-Oxo-2,9-dihydro-1*H*-3-thia-5,9a-diazafluorene-1-carboxylic acid methyl ester (*ortho*-**4**): ^{1}H NMR (300 MHz, $CDCl_3$) δ 3.29 (dd, J = 3.5, 13.2 Hz, 1H), 3.53 (ddd, J = 2.0, 3.3, 13.2 Hz, 1H), 3.74 (s, 3H), 5.52 (dd, J = 3.3, 3.5 Hz, 1H), 6.79 (d, J = 1.8 Hz, 1H), 7.35 (dd, J = 4.9, 7.7 Hz, 1H), 8.11 (dd, J = 1.6, 7.7 Hz, 1H), 8.72 (dd, J = 1.6, 4.9 Hz, 1H). 9-Oxo-8,9-dihydro-7*H*-6-thia-1,8a-diazafluorene-8-carboxylic acid methyl ester (*meta*-**4**): ^{1}H NMR (300 MHz, $CDCl_3$) δ 3.30 (dd, J = 3.4, 13.1 Hz, 1H), 3.53 (ddd, J = 1.5, 3.3, 13.1 Hz, 1H), 3.73 (s, 3H), 5.56 (dd, J = 3.3, 3.4 Hz, 1H), 6.34 (d, J = 1.5 Hz), 7.45 (dd, J = 5.0, 7.7 Hz, 1H), 8.13 (dd, J = 1.5, 7.7 Hz, 1H), 8.78 (dd, J = 1.5, 5.0 Hz, 1H). Anal. Calcd for $C_{12}H_{10}N_2SO_3$ (mixture of regioisomers): C, 54.95; H, 3.84; N, 10.68; S, 12.22. Found: C, 54.88; H, 4.01; N, 10.62; S, 11.82.

Regioisomers **8**: 66% yield, colorless oil. 9-Oxa-2,9-dihydro-1*H*-3-thia-9a-aza-fluorene-1,7-carboxylic acid dimethyl ester (*para*-**8**): ^{1}H NMR (300 MHz, $CDCl_3$) δ 3.30 (dd, J = 3.6, 13.1 Hz, 1H), 3.55 (ddd, J = 1.6, 3.1, 13.1, 1H), 3.77 (s, 3H), 3.96 (s, 3H), 5.54 (dd, J = 3.1, 3.6 Hz, 1H), 6.42 (d, J = 1.6 Hz, 1H), 7.66 (dd, J = 0.7, 8.1 Hz, 1H), 8.27 (dd, J = 1.6, 8.1 Hz, 1H), 8.54 (dd, J = 0.7, 1.6 Hz, 1H); ^{13}C NMR (75.5 MHz, $CDCl_3$) δ 27.8 (t), 50.6 (q), 52.4 (q), 53.2 (d), 102.3 (d), 119.0 (d), 125.2 (d), 127.3 (s), 129.5 (s), 130.2 (s), 133.2 (d), 138.0 (s), 166.0 (s), 168.0 (s). 9-Oxa-2,9-dihydro-1*H*-3-thia-9a-azafluorene-1,6-carboxylic acid dimethyl ester (*meta*-**8**): ^{1}H NMR (300 MHz, $CDCl_3$) δ 3.30 (dd, J = 3.6, 13.1 Hz, 1H), 3.55 (ddd, J = 1.6, 3.1, 13.1 Hz, 1H), 3.77 (s, 3H), 3.98 (s, 3H), 5.54 (dd, J = 3.1, 3.6 Hz, 1H), 6.40 (d, J = 1.6 Hz, 1H), 7.92 (dd, J = 0.8, 8.0 Hz, 1H), 8.13 (dd, J = 1.4, 8.0 Hz, 1H), 8.54 (dd, J = 0.8, 1.4 Hz, 1H); ^{13}C NMR (75.5 MHz, $CDCl_3$) δ 27.8 (t), 50.7 (q), 52.2 (q), 53.2 (d), 101.0 (d), 120.6 (d), 123.4 (d), 129.4 (d), 129.5 (s), 130.2 (s), 134.8 (s), 138.0 (s), 164.9 (s), 168.1 (s). Anal. Calcd for $C_{15}H_{13}NSO_5$ (mixture of regioisomers): C, 56.42; H, 4.10; N, 4.39; S, 10.04. Found: C, 56.72; H, 3.98; N, 4.25; S, 9.72.

Acknowledgment. This work was supported by the Deutsche Forschungsgemeinschaft (projects GR 881/7-2 and 7-3, GU 413/3), the Fonds der Chemischen Industrie, Degussa-Hüls AG, and Bayer AG.

JO001070R